

C-Coll: Introducing Error-bounded Lossy Compression into MPI Collectives

Jiajun Huang
jhuan380@ucr.edu
University of California, Riverside
Riverside, United States of America

Sheng Di
sdi1@anl.gov
Argonne National Laboratory
Lemont, United States of America

Xiaodong Yu
xyu@anl.gov
Argonne National Laboratory
Lemont, United States of America

Yujia Zhai
yzhai015@ucr.edu
University of California, Riverside
Riverside, United States of America

Jinyang Liu
jliu447@ucr.edu
University of California, Riverside
Riverside, United States of America

Ken Raffanetti
raffanet@anl.gov
Argonne National Laboratory
Lemont, United States of America

Hui Zhou
zhouh@anl.gov
Argonne National Laboratory
Lemont, United States of America

Kai Zhao
kzhao@uab.edu
The University of Alabama at
Birmingham
Birmingham, United States of
America

Zizhong Chen
chen@cs.ucr.edu
University of California, Riverside
Riverside, United States of America

Franck Cappello
cappello@mcs.anl.gov
Argonne National Laboratory
Lemont, United States of America

Yanfei Guo
yguo@anl.gov
Argonne National Laboratory
Lemont, United States of America

Rajeev Thakur
thakur@anl.gov
Argonne National Laboratory
Lemont, United States of America

ABSTRACT

With the ever-increasing computing power of supercomputers and the growing scale of scientific applications, the efficiency of MPI collective communications turns out to be a critical bottleneck in large-scale distributed and parallel processing. Large message size in MPI collectives is a particularly big concern because it may significantly delay the overall parallel performance. To address this issue, prior research simply applies the off-the-shelf fix-rate lossy compressors in the MPI collectives, leading to suboptimal performance, limited generalizability, and unbounded errors. In this paper, we propose a novel solution, called *C-Coll*, which leverages error-bounded lossy compression to significantly reduce the message size, resulting in a substantial reduction in communication cost. The key contributions are three-fold. (1) We develop two general, optimized lossy-compression-based frameworks for both types of MPI collectives (collective data movement as well as collective computation), based on their particular characteristics. Our framework not only reduces communication cost but also preserves data accuracy. (2) We customize an optimized version based on SZx, an ultra-fast error-bounded lossy compressor, which can meet the specific needs of collective communication. (3) We integrate *C-Coll* into multiple collectives, such as MPI_Allreduce, MPI_Scatter, and MPI_Bcast, and perform a comprehensive evaluation based on real-world scientific datasets. Experiments show that our solution outperforms the original MPI collectives as well as multiple baselines and related efforts by 3.5–9.7×.

KEYWORDS

Lossy Compression, MPI Collective, Distributed Systems, Scientific Datasets

1 INTRODUCTION

MPI collectives provide high-performance collective communications in distributed systems, making a significant impact on various research fields such as scientific applications, distributed machine learning, and others [1, 2, 4, 5, 16, 30]. With the advent of exascale computing and deep learning applications, the demand for large-message MPI collectives has increased. For example, in image classification tasks, VGG19 [25] and ResNet-50 [14] have 143 million and 25 million parameters, respectively, with communication overheads of 83% and 72% [2]. Therefore, optimizing MPI collectives for large messages has become essential [6, 7, 24].

MPI collectives consist of both internode and intranode communications. The overall collective performance is usually limited by the efficiency of internode communications because of limited network bandwidth. Therefore, optimizing internode collective communication is critical to improving the overall performance of MPI collectives. This has been an active research area for decades, and state-of-the-art algorithms have achieved significant improvements. However, the demand for large-message MPI collectives is growing, and further optimization is necessary [3, 24, 28].

Lossy compression [10, 21, 26, 36] (rather than lossless compression [8, 9, 23]) is a promising solution to mitigate this MPI collective performance issue because of its ability to significantly reduce the message size. Although lossy compression has been widely used to resolve many other scalability issues in high-performance computing, such as reducing memory footprint [31], reducing storage space [19, 37], and avoiding duplicated computation [12], only a few studies have explored its use in this direction, and all expose

certain limitations. To elaborate, Zhou et al. [38] proposed GPU-compression enhanced point-to-point communication by integrating MPC [32] and 1D fixed-rate ZFP [21] into MVAPICH2 [27]. Their approach, referred to as *CPR-P2P*, simply involved compressing the messages before transmission and decompressing them after reception, leading to significant performance overhead due to the non-negligible time required for compression and decompression. In addition, Zhou et al. [39] proposed an approach to improve MPI_Alltoall by using 1D fixed-rate ZFP [21] on GPU. However, their method is closely coupled with the MPI_Alltoall operation, which limits its applicability to other collectives such as MPI_Allreduce. Additionally, both Zhou et al.'s methods rely on fixed-rate compression¹, which introduces two significant issues: (1) compression errors cannot be bounded, leading to uncontrolled accuracy, and (2) the compression quality is considerably lower compared to the fixed-accuracy mode² in ZFP, as demonstrated by prior research [29].

The aforementioned limitations of compression-enabled MPI collective algorithms motivate us to propose a set of highly efficient MPI collectives assisted by error-bounded lossy compression. However, this brings in three direct technical challenges. **A** Devising a general framework that can effectively hide the communication cost and choose an appropriate timing to call lossy compression is non-trivial. **B** The data loss nature of the lossy compression brings up a critical concern on the accuracy of collective operations. **C** Existing lossy compressors are not designed for the collective context, leading to suboptimal collective performance because of unnecessary overheads when they are directly applied in MPI collectives [10, 20, 21, 26, 33].

We propose a novel design (called *C-Coll*) to address the aforementioned limitations and challenges. It integrates error-bounded lossy compression with MPI collectives to significantly improve their performance while maintaining bounded errors. To the best of our knowledge, this is the first-ever framework that provides a general high-performance solution for compression-integrated MPI collectives. Moreover, this is the first accuracy-aware design that ensures that the accelerated collective performance with lossy compression does not compromise data quality. To be more specific, our contributions include:

- To address challenge **A**, we present two frameworks for compression-integrated MPI collectives to significantly diminish the compression overhead in the collective data movement operations and hide communication inside of compression in collective computation collectives.
- To address challenge **B**, we carefully control the number of compression operations and also devise an efficient method that can resolve the unbalanced collective communication issue introduced by the error-bounded lossy compression.
- To address challenge **C**, we customize an optimized version based on SZx to meet the specific needs of collective communication. Specifically, we reduce the number of buffer allocations, implement pipelined SZx to overlap compression

and communication, and resolve the memset problem in the original SZx to achieve better performance, particularly in multithreaded cases. Moreover, we carefully integrate multithreaded SZx with MPI to better utilize modern hardware and achieve higher compression throughput and collective performance.

- To demonstrate the generality of our design, we integrate *C-Coll* into multiple collectives, such as MPI_Allreduce, MPI_Scatter, and MPI_Bcast, and evaluate the performance carefully with various scientific datasets generated by real-world applications. Experiments with 128 Xeon Broadwell compute nodes from a supercomputer show that other related efforts or baselines exhibit undesired performance degradation on MPI_Allreduce because of the significant compression overhead. In comparison, our solution—the lossy-compression-based Allreduce (we call it C-Allreduce)—outperforms the original MPI_Allreduce by 3.5×. Moreover, our compression-based scatter and Bcast operations (namely C-Scatter and C-Bcast) achieve up to 7.7× and 9.7× performance improvements compared with the original MPI_Scatter and MPI_Bcast. We also use a real-world use-case (image stacking analysis) to validate the practical effectiveness of C-Allreduce, which shows up to 2.8× performance gain over MPI_Allreduce, while preserving a high data integrity/accuracy during the collective operations.

The rest of the paper is organized as follows: we introduce the background and related work in Section 2 and then detail our designs and optimizations in Section 3. Evaluation results are presented in Section 4 followed by conclusions in Section 5.

2 BACKGROUND AND RELATED WORK

In this section, we discuss the background and related work.

2.1 MPI Collective Communication

There are many types of MPI collective operations, which can be divided into two sub-categories — collective data movement and collective computation according to their communication patterns.

2.1.1 Collective data movement. Collective data movement includes gather, allgather, scatter, all-to-all, and so on. The gather operation collects the data from different processes and stores the collected data into the root process. In comparison, allgather stores the collected data to every participated process. As an opposite of gather, the scatter operation divides the data in the root process and sends the split data to all the processes. The all-to-all operation acts as the "allscatter", which collectively scatters the data on each process to each other.

2.1.2 Collective computation. Allreduce/reduce are two popular collective computation operations. We use MPI_SUM as an example to explain the working principle as it is frequently used. The reduce routine will sum up all the data entries from all the processes in the same communicator and store the sum into the root process. The Allreduce does the same thing but keeps a copy of the sum on every process in that communicator. Another widely-used operation is the reduce-scatter, which acts like a combination of the reduce and scatter: the reduced sum is scattered into all the processes.

¹Fixed-rate compression means that the lossy compression would be performed based on a user-specified fixed compression ratio.

²Fixed-accuracy, also known as error-bounded lossy compression, compresses data based on a user-specified error bound.

2.2 High-speed Compressors

In general, there are two categories of high-speed data compression methods, namely, lossless and lossy compression, with a particular emphasis on their compression speed.

2.2.1 Lossless compressors. High-speed lossless compressors have been developed to meet the strong demand for compression performance in various use cases. One outstanding lossless compressor is Facebook’s Zstd [8]. Zstd was designed for the purpose of high performance in particular while yielding similar compression ratios compared with other top-performing lossless compressors like Zlib [23] and Gzip [9]. Studies [8] show that Zstd is generally 5-6× faster than Zlib does and has been integrated into over 80 production-level software, libraries, and platforms. However, Zstd is limited to lossless compression, which leads to very low compression ratios (typically 1.2-2) when compressing scientific datasets which primarily are composed of floating-point numbers [33].

2.2.2 Lossy compressors. Compression developers and scientific researchers have shown great interest in high-speed lossy compression due to its ability to achieve a very high compression ratio. SZ [10, 20, 26] is an example of a fast, error-bounded lossy compressor that offers performance similar to other compressors, including FPZIP [22] and SZauto [36]. Another compressor that is known for its relatively high compression ratios and even faster compression speed than SZ is ZFP [21]. However, neither of these compressors can match the speed of SZx [33], which achieves a compression throughput of 700-900 MB/s on CPUs [33]. As such, we developed our customized compressor for MPI collectives based on SZx, which will be detailed in Section 3.2.

2.3 Compression-enabled MPI Implementations

Researchers have shown interest in using compression to improve MPI communication performance for years. Ke et al. [18] and Filgueira et al. [11] have used runtime compression to boost MPI communication performance on CPUs. However, their approaches are restricted to lossless compression that sacrifices the compression ratio for a high compression quality. In contrast, our error-bounded lossy compression enabled MPI collectives not only ensure a satisfying compression quality but also a much higher compression ratio than the lossless ones. Therefore, we conclude that these works are orthogonal to ours. On the other hand, as discussed previously in the introduction, Zhou et al. proposed GPU-compression enhanced point-to-point communication [38] and an optimized MPI_Alltoall operation [39] using 1D fixed-rate ZFP [21] on GPUs, but their solutions are either tightly coupled with the specific collective operations or subject to the fixed-rate mode compression, leading to the inferior compression quality.

3 C-COLL DESIGN AND OPTIMIZATION

Here, we present the design and optimization strategies for *C-Coll*.

3.1 Two Proposed Novel Frameworks for Compression-enhanced Collectives

To integrate lossy compression into MPI collective communications, at least two important aspects must be considered: performance and accuracy. In general, MPI collective operations can be divided

into two groups: collective data movements, and collective computation. Instead of directly using the CPR-P2P method, we propose two frameworks to implement collective communications for each group, which can maximize the collective operation performance.

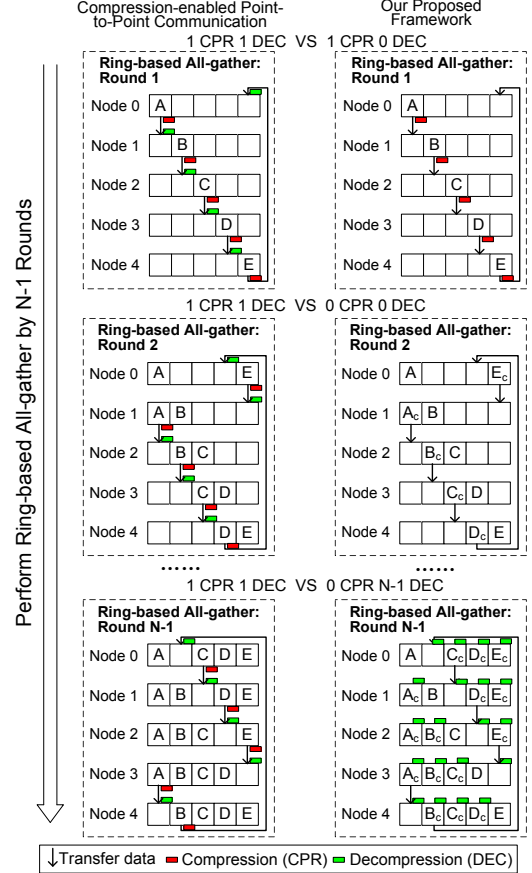


Figure 1: High-level design of our collective data movement framework in the ring-based allgather algorithm. *A* means the original data and *A_c* means the compressed data. This rule applies to other data chunks as well. This algorithm completes in $N-1$ rounds, where N is the number of processes.

3.1.1 Collective data movement framework. In this subsection, we describe how we resolve the communication unbalance issue and compression overhead issue in our optimized collective data movement framework. For collective data movement operations, each process in the same communicator needs to communicate with each other to exchange data. If we directly use the CPR-P2P method, the sender needs to compress the data every time before sending it, and the receiver is required to decompress the data upon the data arrival. Most of the compression and decompression overheads in CPR-P2P, actually, can be avoided by carefully setting the timing of compression operations, as the original data have not been modified during the intensive communications. Besides, the CPR-P2P can cause unbalanced communications in that input data on different processes have various compressed data sizes. Such unbalanced

communication will slow down the overall collective performance, resulting in a sub-optimal performance. With our framework, we can balance the communications with a fixed pipeline size as the compressed data sizes are decided at the beginning of the intensive communications. In the following text, we illustrate our idea with two examples: a ring-based allgather algorithm and a binomial tree broadcast algorithm. The same philosophy can be easily extended to other collective algorithms in this category.

Figure 1 shows the high-level comparison of our proposed framework versus the CPR-P2P in the ring-based allgather algorithm. In this algorithm, the original data are divided into N chunks on each process and $N-1$ rounds are required to get the gathered results on every process, where N is the number of processes in the communicator. Unlike CPR-P2P, our design does not decompress the received data before the last round, thus significantly decreasing the compression overhead from $(N-1) \cdot T_{chunk}$ to T_{chunk} , where T_{chunk} is the compression cost of one chunk. When N is large, our novel framework could have nearly $N \times$ better performance compared with CPR-P2P in terms of compression.

Figure 2 presents a similar comparison in the binomial tree broadcast algorithm, where N refers to the total process count. We notice that our proposed framework could reduce the compression cost from $\log_2 N \cdot (T_{comp} + T_{decomp})$ to $T_{comp} + T_{decomp}$ and the performance improvement is $\log_2 N \times$, where T_{comp} and T_{decomp} are the compression time and decompression time of the data at the root process, respectively.

Apart from the compression cost, the CPR-P2P method brings accumulated errors along with the collective sends and receives because the same chunk of data is compressed and decompressed many times. Our framework also solves the accuracy issue by compressing the same data chunk for only one time. Similar to the analysis of compression overhead, for the absolute error bounded compression, our proposed framework can decrease the accuracy loss by $(N-1) \times$ and $(\log_2 N) \times$ in the ring-based allgather and binomial tree broadcast algorithm, respectively.

3.1.2 Collective computation framework. For collective computation routines, the data entries from all processes in the same communicator need to collectively compute with each other. In comparison with the collective data movement case, the transferred data can be updated in this communication pattern. As a result, the previous framework cannot be utilized here thus we need to propose a new framework. Because of the necessity of computation, we cannot diminish the compression, however, we find an opportunity to hide communication inside the compression and decompression. To clearly elaborate our proposed design, we use the ring-based reduce_scatter algorithm as an instance. Note that this framework can be easily extended to other collective computation operations.

Our proposed framework for collective computation is illustrated in Figure 3. In the ring-based reduce_scatter algorithm, each process must send and receive message chunks to and from its neighbors. The chunk size can be quite large for large input data, as it equals the input data size divided by the number of processes. In the original CPR-P2P, compression and decompression occur before and after any communication. As a result, a single round entails three types of costs, including compression/decompression costs for

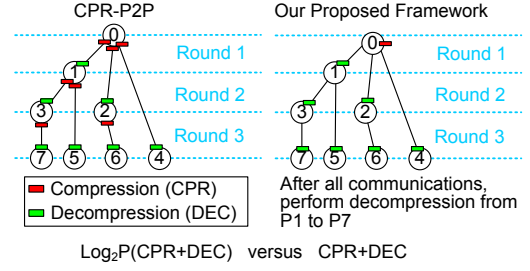


Figure 2: High-level design of our collective data movement framework in the binomial tree broadcast algorithm. It completes in $\log_2 N$ rounds, where N is the number of processes.

one message chunk, send/receive costs for the compressed message chunk, and reduction costs for one message chunk. In our proposed design, we hide the send/receive costs in the compression and decompression phases by actively pulling communication progress inside the compression/decompression phases, which significantly reduces communication time.

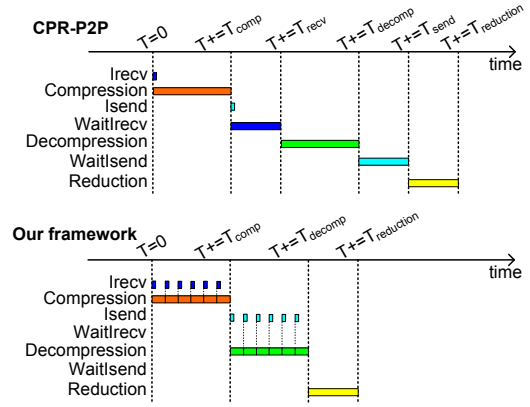


Figure 3: High-level design of our collective computation framework in the ring-based reduce-scatter algorithm.

3.2 Identify Best-qualified High-speed Lossy Compressor

In this section, we compare various lossy compressors and select the most suitable one for MPI collectives. As shown in the previous analysis, in addition to controlling the data distortion by error bounds, the compression throughput and compression ratio are two critical metrics to consider. According to the prior literature [10, 20, 33, 34, 36], ZFP and SZx exhibit much higher compression speed than other compressors, including SZ2 [20], SZ3 [34], FPZIP [22], and Auto-SZ [36]. Therefore, we focus on ZFP and SZx in particular and select the best-qualified one for compression-enabled collective communication. In ZFP, users can set a fixed compression rate in the fixed-rate (FXR) mode or a fixed absolute error bound in the fixed-accuracy (ABS) mode. The two modes have their particular pros and cons. The advantage of the FXR is that it brings up substantial convenience in some use cases that require knowing the compressed data size in advance. In comparison with FXR mode, ZFP's ABS mode features a much higher compression quality on

scientific datasets (i.e., higher compression ratio with the same reconstructed data quality), as verified in [29]. We briefly analyze the key reason why ZFP’s ABS mode has higher compression quality than its FXR mode in the following text. ZFP divides the dataset into small data blocks during the compression. Unlike ZFP(ABS) which allows variable compressed size for each block, ZFP(FXR) strictly forces each block to have the same compression ratio, which may inevitably degrade the quality of reconstructed data in turn. Moreover, the FXR mode cannot control the error bound, which may cause fairly high compression errors on some data points unexpectedly. In comparison with ZFP, SZx is an ultra-fast error-bounded compressor that was designed driven by the fixed-accuracy mode.

Table 1: OVERALL COMPRESSION/DECOMPRESSION THROUGHPUT (MB/S)

Datasets		RTM		Hurricane		CESM-ATM	
SZx	ABS	Com	Decom	Com	Decom	Com	Decom
	1E-2	1742	3309	1687	3640	666	1251
	1E-3	1479	2723	895	1659	533	918
	1E-4	1288	2215	644	1168	526	822
ZFP(ABS)	ABS	Com	Decom	Com	Decom	Com	Decom
	1E-2	1383	1444	492	634	240	273
	1E-3	1082	1141	307	397	170	191
	1E-4	783	811	170	209	128	136
ZFP(FXR)	FXR	Com	Decom	Com	Decom	Com	Decom
	4	610	601	251	319	335	397
	8	438	413	129	142	200	203
	16	324	311	82	81	119	112

Table 2: COMPRESSION RATIOS (ORIGINAL DATA SIZE / COMPRESSED DATA SIZE)

Datasets		RTM			Hurricane			CESM-ATM		
SZx	ABS	min	avg	max	min	avg	max	min	avg	max
	1E-2	88	116.3	124.1	121	123.1	124.1	4.9	8.5	22.8
	1E-3	26.1	49.4	115.1	14.9	17.4	29.1	3.3	5.1	13.1
	1E-4	9.5	30.4	111.3	6.9	7.2	8.8	2.4	3.4	8
ZFP(ABS)	ABS	min	avg	max	min	avg	max	min	avg	max
	1E-2	67.7	87.6	125.2	18.1	18.3	18.6	4.7	8.1	23.1
	1E-3	30.6	58.4	123.2	10.5	10.7	11	3.4	5.6	15
	1E-4	13.4	38	120.1	5.4	5.5	5.8	2.4	3.8	9.7
ZFP(FXR)	FXR	min	avg	max	min	avg	max	min	avg	max
	4	8	8	8	8	8	8	8	8	8
	8	4	4	4	4	4	4	4	4	4
	16	2	2	2	2	2	2	2	2	2

Table 3: COMPRESSION QUALITIES (PSNR)

Datasets		RTM			Hurricane			CESM-ATM		
SZx	ABS	min	avg	max	min	avg	max	min	avg	max
	1E-2	31.2	37.3	61.5	25.2	26.2	26.8	46	50.6	55.9
	1E-3	40.6	51.4	80.9	40.3	42	42.8	64.2	70.3	73.4
	1E-4	60.2	72	102.6	62.4	63.6	64.3	82.8	93.5	97.2
ZFP(ABS)	ABS	min	avg	max	min	avg	max	min	avg	max
	1E-2	36.6	45.7	71.8	33	34	34.3	52.6	56.8	61
	1E-3	49.2	59.5	88.2	47.8	49	50	69.1	73.2	77.6
	1E-4	69.3	80.1	111	68.5	69.7	70.4	92.2	96.6	100.6
ZFP(FXR)	FXR	min	avg	max	min	avg	max	min	avg	max
	4	41.9	46.4	56.1	30.9	31.6	32.3	30.3	34	39.9
	8	66.7	71.6	80.1	56	57.8	64.9	58.8	60.5	62.9
	16	113.8	118.5	127.3	103.7	105.5	113	106.4	108.1	110.6

In addition to the above analysis, we also compare SZx, ZFP(ABS), and ZFP(FXR) regarding the compression throughput, ratio, and

quality, using different datasets with various error bounds or rates, as shown in Table 1, 2, and 3. For fairness, all compression and decompression operations were performed with a single thread on the Intel Xeon E5-2695v4 CPU. We adopt the 1D compression mode in that the dimensional information will have to be skipped due to the 1D chunk-wise design in most of the MPI collectives. The information about the datasets we used here is detailed in Table 4, which will be found in Section 4.1. Because of the space limit, we use the QVAPORF and CLOUD fields in the Hurricane and CESM-ATM dataset, respectively, in our experiments, and other fields exhibit very similar results. We observe that SZx is much faster than ZFP(ABS) by up to 4.1 \times in compression and 5.7 \times in decompression with similar compression ratios and qualities. Additionally, with similar compression qualities, ZFP(FXR) has the lowest compression speed and compression ratio compared to both ZFP(ABS) and SZx. Therefore, we develop our customized compressor based on SZx in terms of the context of MPI collectives. For the purpose of comparison, we also implement compression-enabled point-to-point communication-based collectives based on both ZFP(FXR) and ZFP(ABS), which serve as baselines.

3.3 Characterization of Performance Bottlenecks

We integrate SZx into point-to-point communication of the ring-based allreduce algorithm, in order to understand the key bottlenecks of the collective performance, which will be a fundamental work to guide our optimization strategies. In this characterization, we use ring-based allreduce which serves as a very good example, because it consists of both collective data movement (allgather) and collective computation (reduce_scatter). Figure 4 presents the detailed performance breakdown for direct integration of SZx under a series of data sizes. Our analysis reveals that in the original ring-based allreduce algorithm, the all-gather operation accounts for approximately 60% of the overall execution time, as the communications are not overlapped at all with each other, unlike the reduce-scatter stage. The Wait operation is the second most time-consuming one, which waits for the completion of non-blocking send and receives before conducting the reduction operation. The remaining operations in the original allreduce algorithm include Memcpy (local data copies), Reduction (Reduce operations), and Others (data allocations and other calculations), which together constitute about 20% of the overall execution time. After integrating the SZx, the bottleneck turns the ComDecom (compression and decompression) as the data needs to be compressed before being sent out and needs to be decompressed everytime the receiver receives them. We also observe a reduction in Allgather and Wait times, suggesting a decrease in transferred data, and both of the MPI-related time can be further optimized. However, the Others part also takes a significant amount, specifically 23% in the 278MB case. This is because the SZx requires users to free compression-generated buffers after the compressor is called, resulting in a significant overhead.

3.4 Step-wise Optimizations

In this subsection, we describe our step-wise optimization strategies, which is a key contribution of this paper. For the convenience of description, we present our implemented ring-based allreduce

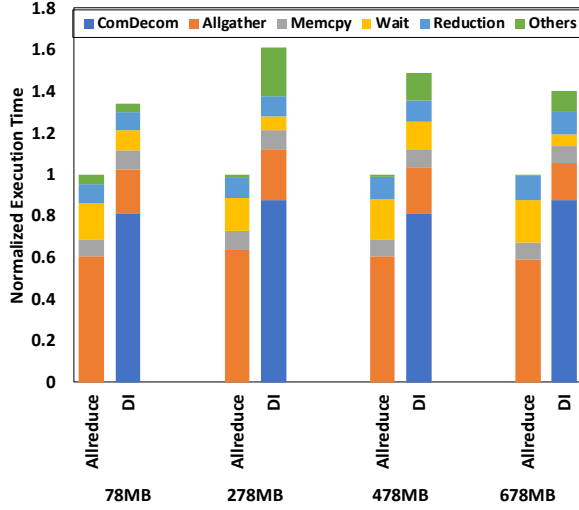


Figure 4: Compare the performance of Allreduce(Original MPI_Allreduce) and the DI(Direct Integration) of SZx from 78MB to 678MB with 200MB step.

that enables lossy compression, and the optimization strategies are also applied to other collectives. What is more, the data transaction for each process is only $\frac{2(N-1)}{N} \cdot D_{input}$ in the ring-based allreduce algorithm, where D_{input} is the input data size and N is the process count. Such a design is supposed to be very efficient for long messages. Moreover, our enabled lossy compression capability can also significantly benefit the collective communication with long messages. We name our designed lossy-compression enabled MPI_Allreduce as C-Allreduce, where C means compression. In the following text, we discuss our design and implementation details of the proposed C-Allreduce in a step-wise manner.

3.4.1 Utilize our collective data movement framework. To reduce the compression overhead and balance communications, we utilize the data movement framework that we presented in Section 3.1.1. At the beginning, every process compresses its local data and stores the compressed data size. Then, every process synchronizes with each other to collect the compressed data sizes in a local integer array *compressed_sizes*. As the compressed data size only has four bytes, this step is very fast. After that, all processes get the sum of all the compressed data sizes, noted as *total_count*. Then, each process communicates with each other with a fixed pipeline size until every process has sent $to_send = total_count - compressed_sizes[send_rank]$ and received $to_recv = total_count - compressed_sizes[self_rank]$ from other processes in a ring communication pattern. After all communications end, every process starts to decompress all the received compressed data and store the decompressed data in the receive buffer. Note that they do not need to decompress the data that are compressed by themselves. After this step, we can significantly decrease the time spent by compression and allgather communications compared with the direct integration of SZx. Besides, our solution can also preserve the quality/accuracy of the data very well because of the error-bounding feature, which will be demonstrated later in Section 4.5.

3.4.2 Redesign buffer allocation and data initialization. To meet the requirements of collective communications, we need to optimize and customize SZx to have better performance. In SZx, the original data and its size information are passed into the compression kernel, in which a set of buffers (such as stateArray, medianArray, and radiusArray) are created to process the original data. After the compression, the kernel returns a pointer to the compressed data buffer, which is also initialized inside of SZx. Even worse, the compressed data needs to be freed in time for each compression (otherwise, the whole memory would be used up very quickly, leading to a crash), which also introduces a certain cost. Since SZx needs to be called multiple times in the entire collective operation, there would be many redundant buffer allocations and data initialization, which may significantly delay the overall performance unexpectedly. To verify the potentially huge cost of memory allocation and data initialization in SZx, we perform a performance breakdown. We find that the buffer allocation and data initialization may take over 50% of the overall execution time of single-threaded SZx. The situation could be even worse for a multi-threaded SZx as the buffer allocation and data initialization cannot be parallelized. To solve this issue, we carefully remove most of the compression-related buffer allocations and data initialization inside of SZx and pre-allocate them only once in the entire collective algorithm and reuse them upon need. We call this solution *optimized SZx* (OPT-SZx), based on which we can enormously boost the compression kernel and meanwhile resolve the memory and performance issue caused by the compression buffers.

3.4.3 Customize an optimized version based on SZx to reduce communication overhead with our collective computation framework. In order to use our collective computation framework in the reduce-scatter stage of the ring-based allreduce algorithm, we need to redesign the compression workflow of SZx so that we can consistently poll the progress of the Isend and Irecv inside of the compression and decompression. Therefore, we design and implement the PIPE-SZx (pipelined SZx) based on the OPT-SZx. Instead of compressing the original data as a whole, we divide the compression process into small chunks, each of which handles 5120 data points. Between the compression of two adjacent chunks, we actively poll the communication progress of the non-blocking receive. However, the compressed data of each chunk cannot be simply combined together, otherwise the compressed data cannot be correctly decompressed because each compressed chunk is of variable uncertain length. To solve this problem, we decide to store the compressed data of all chunks in the same output buffer and pre-allocate enough memory space at the front of the buffer for storing the compressed data sizes of those chunks together (essentially a kind of index), instead of storing them along with the compressed data chunks. Such a design is more cache-friendly, thus having lower overhead. During the decompression, we maintain a chunk-starting-location pointer based on the recorded compressed chunk sizes to tell the algorithm where the decompression operation should start for each chunk. We repeat this process chunk by chunk and poll the progress of the non-blocking send between decompression chunks. Through this optimization, we can hide the communication in the reduce-scatter stage inside of compression, which further improves the performance of our C-Allreduce design.

3.4.4 Improve compression performance with multithreading. As modern CPUs are mainly multi-core machines, the single-thread compression cannot fully utilize the available resources and has a limited throughput. To solve this issue, we decide to further increase the compression performance by utilizing the multi-threaded OPT-SZx, which has a much better scalability than the original SZx because of our improved buffer allocation and data initialization method. In order to mitigate the possible conflicts between the MPI and OpenMP runtime environment, we map one process to one socket and only allow the main thread to do the MPI calls. On the Intel Xeon E5-2695v4 machine that we are testing, there are 18 physical cores per socket. We observe that the performance enhancement brought by the multi-threaded OPT-SZx almost saturates with 15 threads (15 physical cores), so we set the concurrently running threads in the omp parallel region as 15. With this optimization, we are able to better utilize the modern hardware and achieve a higher compression throughput.

4 EXPERIMENTAL EVALUATION

In this section, we present and discuss the evaluation results.

4.1 Experimental Setup

Since inter-node communication is the major bottleneck for collectives as discussed previously, we utilized a 128-node cluster with one process per node in our experiments. Each node is equipped with two Intel Xeon E5-2695v4 Broadwell processors, yielding a total of 36 cores per node. Furthermore, each NUMA node contains 64 GB of DDR4 memory, resulting in a total of 128 GB of memory per node. The nodes are interconnected via the Intel Omni-Path Architecture (OPA) interconnect, providing a maximum message rate of 97 million per second and a bandwidth of 100 Gbps.

Table 4: INFORMATION OF THE SCIENTIFIC DATASETS

Applications	# files	Dimensions	Descriptions
RTM[17]	70	849×849×235	Seismic Wave
Hurricane[15]	48×13	100×500×500	Weather Simulation
CESM-ATM[35]	26×33	1800×3600	Climate Simulation

MPI collectives are common operations used in the simulation analysis. For instance, generating stacking images in RTM (essentially an allreduce sum operation) is a typical real-world example [13], which will be demonstrated at the end of this section. We also utilize various datasets from a series of applications, including the reverse time migration (RTM) dataset, Hurricane dataset, and CESM-ATM dataset, to evaluate our solution. Table 4 shows the detailed specifications of these datasets. Our baselines consist of original MPI collectives in MPICH 4.1.1, MPI collectives implemented by compression-enabled point-to-point communications with SZx, fix-accuracy ZFP, and fix-rate ZFP (version 0.5.5). For our experiments, we adopt a two-stage approach, including a warm-up stage and an execution stage. We conduct 10 runs for each stage and report the average results to present the general performance.

4.2 Step-wise Optimizations to C-Allreduce with Performance Analysis

In this section, we carry out optimizations to our C-Allreduce (C-Coll enhanced Allreduce) integrated with SZx step by step and show

the performance on 16 Broadwell nodes. The ring-based allreduce that we implement contains a reduce-scatter stage and an allgather stage. Thus, we breakdown the total execution time into several parts: ComDecom (i.e., the time needed to compress and decompress data), Allgather (i.e., the time required to transfer data in the allgather stage), Malloc (i.e., the time spent on coping data in the reduce-scatter stage), Wait (i.e., the non-overlapped time spent on transferring data in the reduce-scatter stage), Reduction (i.e., the time required to do reduction operation), and Others (i.e., the time needed to do other data allocation and calculations). We adopt the RTM dataset to demonstrate our step-wise optimizations, which is the largest one among all three representative scientific datasets we evaluate.

4.2.1 Evaluating our collective data movement framework.

Figure 5 shows the performance improvement achieved by our novel design in the allgather stage for data sizes ranging from 28MB to 678MB. This Novel Design (ND) utilizes our collective data movement framework, resulting in a considerable reduction in compression and decompression time, with a speed-up of up to 1.48× at 128MB compared to the Direct Integration (DI) discussed in Section 3.3. Additionally, our balanced communication in Allgather using the ND is up to 7.1× faster than the unbalanced communication in DI at 628MB. We analyze the key reason why our solution can obtain a significant performance improvement as follows. In fact, to overcome the compression bottleneck and balance MPI communications, we utilize our collective data movement framework that pre-compresses the data before transmission and decompresses it after all communications, rather than using expensive compression-enabled point-to-point communication (CPR-P2P) in collective routines. This novel design can significantly reduce the amount of compression required during collective communication. Using CPR-P2P also brings unbalanced communications as the compressed data sizes may vary, but we can balance the communications with a fixed pipeline size in our new design because we do not need to compress the data every time before we send it.

Note that using CPR-P2P may accumulate errors during intensive collective communication, such as ring-based communication, as the same data is repeatedly passed from one process to another. Therefore, we have utilized our new framework to ensure that errors in the final results are bounded, which we discuss in the application evaluation section 4.5.

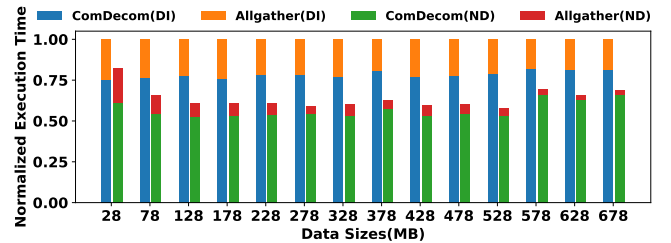


Figure 5: Compare the performance of DI (Direct Integration) and our ND (Novel Design) from 28MB to 678MB.

4.2.2 Evaluating our redesigned buffer allocation and data initialization. Figure 6 presents the performance breakdown comparison of original SZx versus Optimized SZx (OPT-SZx). As shown in Figure 6a, OPT-SZx nearly removes data allocation and initialization cost during the compression as compared with SZx (see the blue bar which represents the Allocate operation). The performance improvement increases further as the number of threads increases: up to 4.8× compared with SZx when running with 15 threads. This is because the Allocate operation in the original compression cannot be parallelized. In Figure 6b, we observe that optimization does not have much impact on decompression as Allocate only takes a small proportion of the original decompression process. Moreover, the performance improvement almost saturates at 15 threads for both compression and decompression.

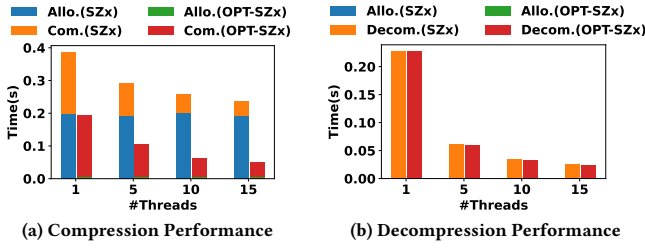


Figure 6: Performance breakdown comparison of SZx (Original SZx) and OPT-SZx (Optimized SZx).

The performance under the new optimization is displayed in Figure 7. As shown in the figure, our OPT-SZx reduces compression/decompression time (ComDecom) by up to 56.4% over the first optimization that was proposed in Section 3.1.1 and evaluated in Section 4.2.1. The OPT-SZx also decreases the time cost on Others by up to 85.3% across all data sizes. This reduction in the Others time is because OPT-SZx no longer generates compressor-related buffers, thereby freeing the program from handling these buffers outside of OPT-SZx. We analyze the reasons behind the performance gain as follows. To further boost the performance of the compression and decompression, we optimize SZx based on the need of collective communications. Therefore, we have significantly reduced the buffer allocations inside SZx and moved the compression-related buffers outside of SZx so that the same buffer can be used for multiple compression and decompression. We also removed unnecessary data initialization to improve its performance.

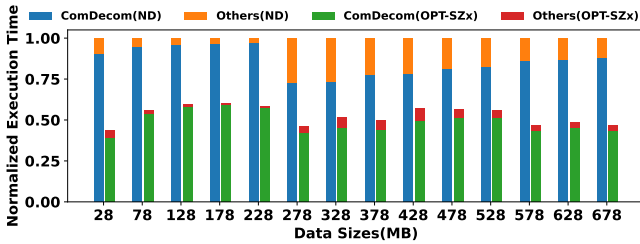


Figure 7: Compare the performance of ND (Novel Design) and OPT-SZx (Optimized SZx) from 28MB to 678MB with a 50MB step.

4.2.3 Evaluating reduced communication overhead with our collective computation framework. We demonstrate the effectiveness of our collective computation framework in this section. From Figure 8, it is evident that the carefully overlapped version (Overlap) leads to significantly less Wait time compared with the previous version (OPT-SZx), resulting in a performance boost of up to 4.9× for the data size of 678MB. The rationale for this performance improvement is shown in the following text. To utilize our collective computation framework for hiding communication during compression, we design and implement PIPE-SZx (pipelined OPT-SZx), which could break the compression process into small chunks and allow us to overlap the compression with communication in a fine-grained pipelined manner. As a result, we can significantly reduce MPI_Wait time in the reduce-scatter stage, which uses non-blocking communications.

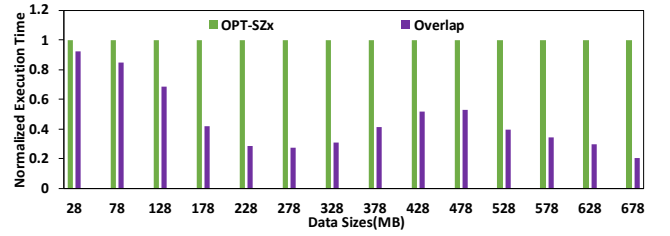


Figure 8: Compare the wait time of OPT-SZx (Optimized SZx) and Overlap (Overlap Optimization) from 28MB to 678MB with a 50MB step.

4.2.4 Evaluating compression performance improvement with multithreading. Figure 9 presents the performance of our multithreaded optimization (Mthread) across different data sizes. The speedup is up to 5.6× when the message size is 528MB, which matches our experimental results in Section 4.2.2. Such a high-performance gain is due to the optimization strategy of combining multithreading (openMP) in the MPI collectives and significantly reducing the relative potential overhead. Specifically, the Intel Xeon E5-2695v4 we are using in our experiment features 18 physical cores per socket. As discussed in Section 4.2.2, the benefit of multithreading would saturate with 15 threads, thus we use 15 threads to enhance the compression performance and carefully integrate the multithreaded version into our framework to avoid potential performance degradation.

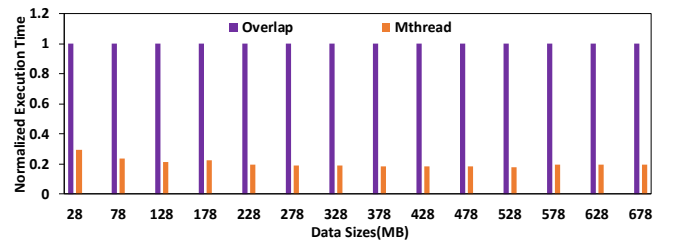


Figure 9: Compare the compression/decompression performance of OPT-Overlap (Overlap Optimization) and Mthread (Multithreading Optimization) from 28MB to 678MB with a 50MB step.

4.3 End-to-end Comparisons of C-Allreduce with Baselines

In this section, we compare the performance of our single-threaded (Ours(1)) and 15-threaded (Ours(15)) C-Allreduce with four different baselines on various data sizes, node numbers, and datasets. The baselines include the original MPI_Allreduce without compression (Allreduce), MPI_Allreduce implemented by compression-enabled point-to-point communication (CPR-P2P) with fixed-rate ZFP (ZFP(FXR)), fixed-accuracy ZFP (ZFP(ABS)), and SZx. The SZx and ZFP(ABS) have a fixed accuracy of $1E-3$, and the ZFP(FXR) has a rate of 4.

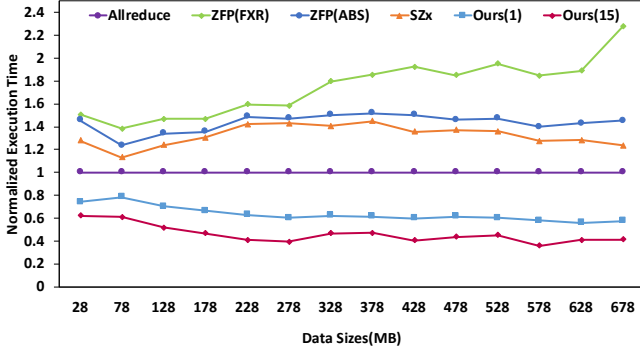


Figure 10: Compare the performance of our C-Allreduce and multiple baselines from 28MB to 678MB with a 50MB step on 128 nodes. Ours(n) means that there are n running threads in our C-Allreduce.

4.3.1 Evaluating with different data sizes on 128 nodes. In this section, we present the performance of our single-threaded and 15-threaded C-Allreduce, along with related baselines, using data sizes ranging from 28MB to 678MB on 128 Broadwell nodes. The RTM dataset is adopted in these experiments. From Figure 10, we can observe that the SZx-integrated baseline performs the best among the three compression-integrated baselines, and ZFP(FXR) has the worst performance. This is because SZx has a faster compression speed compared to ZFP(FXR) and ZFP(ABS). Additionally, ZFP(ABS) and SZx have better compression ratios than ZFP(FXR) as we previously mentioned in 3.2. However, none of the three CPR-P2P baselines can outperform the original Allreduce. By employing our novel framework and step-wise optimizations, our C-Allreduce (referred to as "Ours") achieves significantly higher performance than the original Allreduce in both single-threaded (Ours(1)) and multi-threaded (Ours(15)) cases, with up to $1.8\times$ and $2.8\times$ performance improvements, respectively.

4.3.2 Evaluating with different node numbers with 678MB data. To demonstrate the scalability of our approach, we compare the normalized execution time of our C-Allreduce and four different baselines using a fixed data size of 678MB across 2 to 128 nodes. The RTM dataset is adopted in these experiments. As shown in Figure 11, our C-Allreduce (Ours) outperforms all the baselines across various node numbers. It can reach performance boosts of up to $1.8\times$ and $2.9\times$ in the single-threaded and 15-threaded versions compared to the original Allreduce, respectively. Similar to our observation in Section 4.3.1, we found that all the compressor-integrated baselines

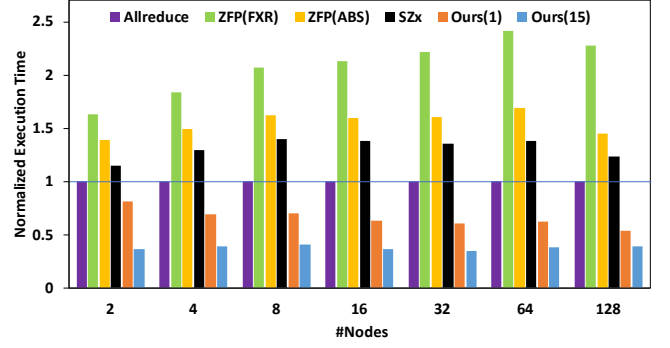


Figure 11: Compare the performance of our C-Allreduce and multiple baselines from 2 to 128 nodes with 678MB message.

exhibit performance degradation compared to the Allreduce, with the SZx-integrated baseline performing the fastest among them.

Table 5: COMPRESSION RATIOS (ORIGINAL DATA SIZE / COMPRESSED DATA SIZE)

Datasets	Hurricane				CESM-ATM
Fields	QVAPORf	PRECIPf	QGRAUPf	CLOUDf	Q
CPR	17.4	88.9	109.6	124.0	105.5

4.3.3 Evaluating with different scientific datasets. In this section, we evaluate the performance of our C-Allreduce and related baselines on different datasets. Due to the page limitation, we only show the SZx baseline here as it has the best performance among compression-enabled baselines. The QVAPORf, PRECIPf, QGRAUPf, and CLOUDf fields are from the Hurricane dataset and the Q field is originated from the CESM-ATM dataset. They have different data distributions and averaged compression ratios as shown in Table 5. From Figure 12, we can notice that our C-Allreduce has the best performance among all the implementations. Specifically, the highest speed-up can be observed in the CLOUDf field, where it is $2.1\times$ and $3.5\times$ faster than the original Allreduce in the single-threaded and 15-threaded modes, respectively. This is because the SZx has the highest compression ratio (124) in CLOUDf. In QVAPORf, we observe that our single-threaded C-Allreduce does not provide the performance gain due to the difficulty in compressing this field, resulting in limited compression throughput and compression ratio (17.4). This low throughput problem has been addressed by our multi-threaded version that can still reach a $1.2\times$ speedup compared to the original Allreduce. However, the fastest compression-enabled baseline (SZx) has performance degradation compared with the original Allreduce due to the limited performance of the CPR-P2P in all cases.

4.4 Generalizability Demonstration on Other MPI Collectives

We have demonstrated the high performance of our C-Allreduce, consisting of C-Allgather and C-Reduce-scatter. To showcase the generalizability of our frameworks and optimizations, we also present C-Bcast and C-Scatter, which utilize the ubiquitous binomial tree algorithm adopted by MPICH. We conduct experiments on the RTM dataset ranging from 28MB to 678MB using 16 Broadwell

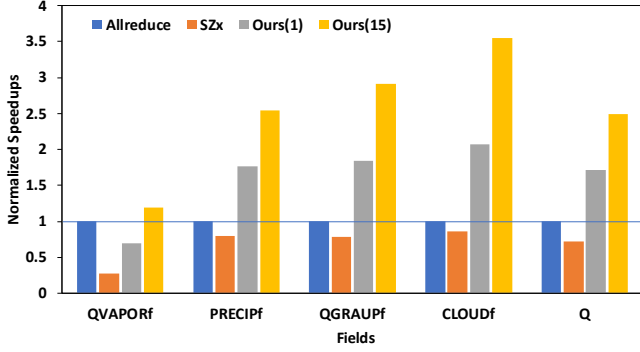


Figure 12: Compare the performance of our C-Allreduce and multiple baselines in different datasets.

nodes. In Figure 13, we present the speedups of our C-Scatter and C-Bcast, normalized against the original MPI_Scatter and MPI_Bcast (Baseline), respectively. We also compare our C-Scatter and C-Bcast with the SZx-integrated CPR-P2P baselines (SZx). Our C-Scatter is 1.8 \times and 7.7 \times faster than Baseline for single-threaded and 15-threaded cases, respectively, while our C-Bcast has up to 2.7 \times and 9.6 \times speedups compared to Baseline for single-threaded and 15-threaded cases, respectively. These performance improvements originated from the decreased data transfer volume and diminished compression overheads from our proposed frameworks. The speedups are even more significant compared to our C-Allreduce because collective data movement benefits more from our frameworks than collective computation. However, the SZx-integrated CPR-P2P baselines are much slower than the baseline due to significant compression overheads.

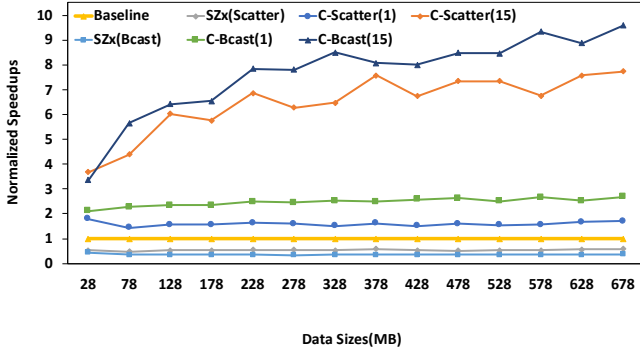


Figure 13: Generalizability demonstration of our proposed framework and optimizations with MPI_Scatter and MPI_Bcast from 28MB to 678MB with a 50MB step.

4.5 Image Stacking Performance Evaluation with Accuracy Analysis

Image stacking is a well-known technique used in various scientific domains, including climate simulation and geology, to generate high-quality images by combining different images. For example, MPI is used by researchers to sum the individual images into final images [13]. In this experiment, we conduct image stacking of the RTM dataset on 16 nodes. As each snapshot has different value

ranges, we use the fixed-accuracy (ABS) mode to compress the data so that each snapshot contributes a similar amount of errors rather than letting the snapshots with large value ranges dominate the errors. Three absolute error bounds (i.e., 1E-2, 1E-3, and 1E-4) are selected to demonstrate the flexibility between the accuracy and performance of our C-Allreduce. The same error bounds are used for the baseline SZx and ZFP(ABS). For ZFP(FXR), three fixed rates (4, 8, and 16) are selected and the related compression ratios are 8, 4, and 2.

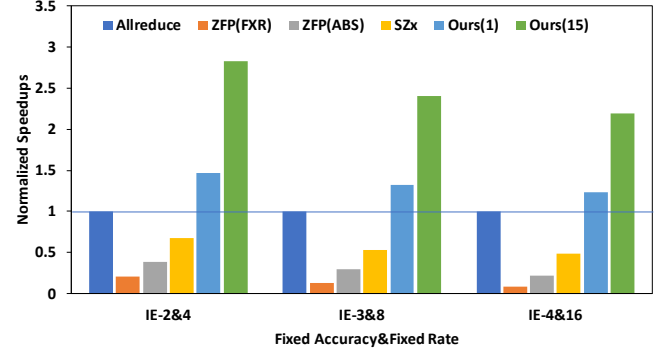


Figure 14: Compare the image stacking performance of our C-Allreduce and multiple baselines in different error bounds for SZx and ZFP(ABS) and rates for ZFP(FXR).

We show the performance results and the visualizations of the stacked images in Figures 14 and 15, respectively. For our C-Allreduce, we could see that, with the increase of error bounds, the performance drops but the quality of the reconstructed image rises. The highest speedup can be witnessed in the 1E-2 case, where our single-threaded and 15-threaded C-Allreduce have 1.5 \times and 2.8 \times higher performance compared to the original Allreduce, respectively. Nevertheless, the three compression-integrated baselines (i.e., SZx, ZFP(ABS), and ZFP(FXR)) all result in performance degradation compared with the original Allreduce, regardless of the absolute error bounds or rates. With an error bound of 1E-4, our C-Allreduce shows an excellent reconstructed image quality, whereas the ZFP(ABS) integrated baseline with the same error bound cannot achieve the same quality. This is because that our proposed frameworks can significantly decrease the accuracy loss of the reconstructed data, while the CPR-P2P cannot. Due to the page limitation, we do not show the reconstructed image of the SZx integrated baseline as it has even worse quality compared with ZFP(ABS). Besides, the ZFP(FXR) baseline with a rate of 4 has the worst reconstructed quality and the stacked image is completely different from the original one, as the fixed-rate mode cannot ensure a bounded accuracy. In a nutshell, our C-Allreduce integrated with our proposed frameworks can remarkably increase the performance of the original Allreduce and also preserves the quality of the original datasets.

5 CONCLUSIONS

In this paper, we introduce *C-Coll*, a novel design for lossy-compression-integrated MPI collectives that significantly improves performance with bounded errors. Our two proposed high-performance

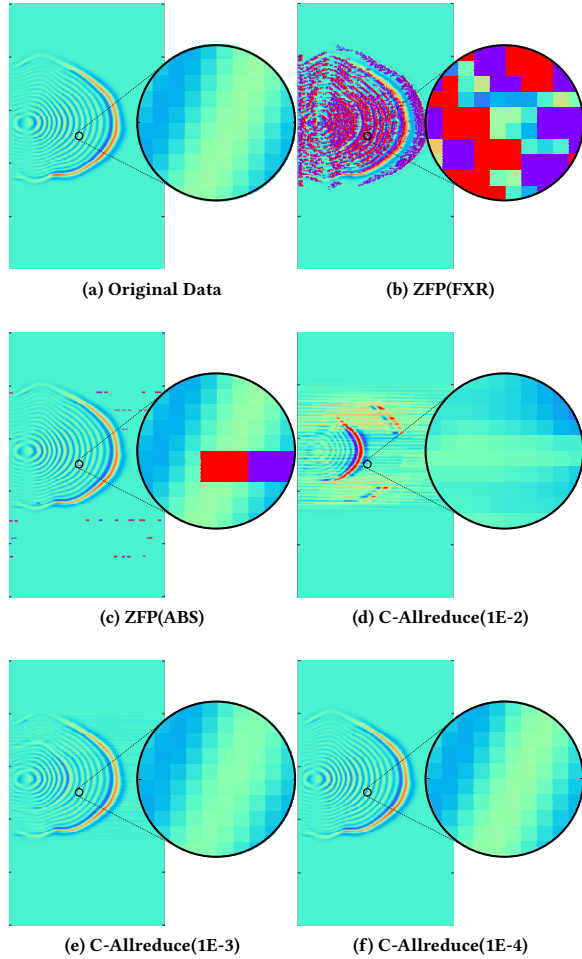


Figure 15: Compare the reconstructed image qualities of our C-Allreduce with different ZFP-integrated baselines.

frameworks for compression-integrated MPI collectives, together with optimized and customized SZx, enable us to implement C-Allreduce, which outperforms the original Allreduce by up to 3.5× while preserving high data quality. We demonstrate the generalizability of our approaches through C-Scatter and C-Bcast, which outperform the original MPI_Scatter and MPI_Bcast by up to 7.7× and 9.7×, respectively. In summary, our research has addressed the issues of sub-optimal performance, lack of generality, and unbounded errors in lossy-compression-integrated MPI collectives, laying the foundation for future research in this area. Moving forward, we plan to expand our research by implementing more C-Coll based collectives and deploying our frameworks and optimizations on other hardware, such as GPUs and AI accelerators.

ACKNOWLEDGMENT

This research was supported by the Exascale Computing Project (ECP), Project Number: 17-SC-20-SC, a collaborative effort of two DOE organizations — the Office of Science and the National Nuclear Security Administration, responsible for the planning and preparation of a capable exascale ecosystem, including software, applications, hardware, advanced system engineering and early

testbed platforms, to support the nation’s exascale computing imperative. The material was supported by the U.S. Department of Energy, Office of Science, Advanced Scientific Computing Research (ASCR), under contract DE-AC02-06CH11357, and supported by the National Science Foundation under Grant OAC-2003709, OAC-2104023. We acknowledge the computing resources provided on Bebop (operated by Laboratory Computing Resource Center at Argonne).

REFERENCES

- [1] Martin Abadi, Paul Barham, Jianmin Chen, Zhifeng Chen, Andy Davis, Jeffrey Dean, Matthieu Devin, Sanjay Ghemawat, Geoffrey Irving, Michael Isard, et al. 2016. Tensorflow: A system for large-scale machine learning. In 12th {USENIX} symposium on operating systems design and implementation ({OSDI} 16). 265–283.
- [2] Ahmed M. Abdelmoniem, Ahmed Elzanaty, Mohamed-Slim Alouini, and Marco Canini. 2021. An Efficient Statistical-based Gradient Compression Technique for Distributed Training Systems. arXiv:2101.10761 [cs.LG]
- [3] George Almási, Philip Heidelberger, Charles J. Archer, Xavier Martorell, C. Chris Erway, José E. Moreira, B. Steinmacher-Burow, and Yili Zheng. 2005. Optimization of MPI Collective Communication on BlueGene/L Systems. In *Proceedings of the 19th Annual International Conference on Supercomputing* (Cambridge, Massachusetts) (ICS '05). Association for Computing Machinery, New York, NY, USA, 253–262. <https://doi.org/10.1145/1088149.1088183>
- [4] Ammar Ahmad Awan, Khaled Hamidouche, Jahanzeb Maqbool Hashmi, and Dhableswar K Panda. 2017. S-caffe: Co-designing mpi runtimes and caffe for scalable deep learning on modern gpu clusters. In *Proceedings of the 22nd ACM SIGPLAN Symposium on Principles and Practice of Parallel Programming*. 193–205.
- [5] Alan Ayala, Stanimire Tomov, Xi Luo, Hejer Shaeik, Azzam Haidar, George Bosilca, and Jack Dongarra. 2019. Impacts of Multi-GPU MPI collective communications on large FFT computation. In *2019 IEEE/ACM Workshop on Exascale MPI (ExaMPI)*. IEEE, 12–18.
- [6] M. Bayatpour and M. A. Hashmi. 2018. SALaR: Scalable and Adaptive Designs for Large Message Reduction Collectives. In *2018 IEEE International Conference on Cluster Computing (CLUSTER)*. 1–10. <https://doi.org/10.1109/CLUSTER.2018.00009>
- [7] Sudheer Chunduri, Scott Parker, Pavan Balaji, Kevin Harms, and Kalyan Kumar. 2018. Characterization of mpi usage on a production supercomputer. In *SC18: International Conference for High Performance Computing, Networking, Storage and Analysis*. IEEE, 386–400.
- [8] Y. Collet. 2015. Zstandard – real-time data compression algorithm. <http://facebook.github.io/zstd/>.
- [9] L. P. Deutsch. 1996. GZIP file format specification version 4.3. <https://datatracker.ietf.org/doc/draft-deutsch-gzip-spec/03/>.
- [10] Sheng Di and Franck Cappello. 2016. Fast error-bounded lossy HPC data compression with SZ. In *2016 IEEE International Parallel and Distributed Processing Symposium (IPDPS)*. IEEE, 730–739.
- [11] Rosa Filgueira, David Expósito Singh, Alejandro Calderón, and Jesús Carretero. 2009. CoMPI: Enhancing MPI Based Applications Performance and Scalability Using Run-Time Compression. In *PVM/MPI*.
- [12] Ali Murat Gok, Sheng Di, Yuri Alexeev, Dingwen Tao, Vladimir Mironov, Xin Liang, and Franck Cappello. 2018. PaSTRI: Error-Bounded Lossy Compression for Two-Electron Integrals in Quantum Chemistry. In *2018 IEEE International Conference on Cluster Computing (CLUSTER)*. 1–11. <https://doi.org/10.1109/CLUSTER.2018.00013>
- [13] Jérôme Gurhem, Henri Calandra, and Serge G. Petiton. 2021. Parallel and Distributed Task-Based Kirchhoff Seismic Pre-Stack Depth Migration Application. In *2021 20th International Symposium on Parallel and Distributed Computing (ISPD)*. 65–72. <https://doi.org/10.1109/ISPD52870.2021.9521599>
- [14] Kaiming He, Xiangyu Zhang, Shaoqing Ren, and Jian Sun. 2016. Deep residual learning for image recognition. *Proceedings of the IEEE conference on computer vision and pattern recognition* (2016), 770–778.
- [15] Hurricane ISABEL simulation data. 2004. <http://vis.computer.org/vis2004contest/data.html>. Online.
- [16] Arpan Jain, Ammar Ahmad Awan, Hari Subramoni, and Dhableswar K Panda. 2019. Scaling tensorflow, pytorch, and mxnet using mvapich2 for high-performance deep learning on frontera. In *2019 IEEE/ACM Third Workshop on Deep Learning on Supercomputers (DLS)*. IEEE, 76–83.
- [17] Suha Kayum et al. 2020. GeoDRIVE – a high performance computing flexible platform for seismic applications. *First Break* 38, 2 (2020), 97–100.
- [18] Jian Ke, M. Burtcher, and E. Speight. 2004. Runtime Compression of MPI Messages to Improve the Performance and Scalability of Parallel Applications. In *SC '04: Proceedings of the 2004 ACM/IEEE Conference on Supercomputing*. 59–59.

- <https://doi.org/10.1109/SC.2004.52>
- [19] Sihuan Li, Sheng Di, Xin Liang, Zizhong Chen, and Franck Cappello. 2018. Optimizing Lossy Compression with Adjacent Snapshots for N-body Simulation Data. In *2018 IEEE International Conference on Big Data (Big Data)*. 428–437. <https://doi.org/10.1109/BigData.2018.8622101>
 - [20] Xin Liang, Sheng Di, Dingwen Tao, Sihuan Li, Shaomeng Li, Hanqi Guo, and Franck Cappello. 2018. Error-Controlled Lossy Compression Optimized for High Compression Ratios of Scientific Datasets. 438–447. <https://doi.org/10.1109/BigData.2018.8622520>
 - [21] Peter Lindstrom. 2014. Fixed-Rate Compressed Floating-Point Arrays. *IEEE Transactions on Visualization and Computer Graphics* 20 (2014), 2674–2683.
 - [22] Peter Lindstrom and Martin Isenburg. 2006. Fast and Efficient Compression of Floating-Point Data. *IEEE Transactions on Visualization and Computer Graphics* 12, 5 (sep 2006), 1245–1250. <https://doi.org/10.1109/TVCG.2006.143>
 - [23] Jean loup Gailly and Mark Adler. [n. d.]. zlib. <https://www.zlib.net/>.
 - [24] Pitch Patarasuk and Xin Yuan. 2009. Bandwidth optimal all-reduce algorithms for clusters of workstations. *J. Parallel and Distrib. Comput.* 69, 2 (2009), 117–124.
 - [25] Karen Simonyan and Andrew Zisserman. 2015. Very deep convolutional networks for large-scale image recognition. *arXiv preprint arXiv:1409.1556* (2015).
 - [26] Dingwen Tao, Sheng Di, and Franck Cappello. 2017. Significantly Improving Lossy Compression for Scientific Data Sets Based on Multidimensional Prediction and Error-Controlled Quantization. <https://doi.org/10.1109/IPDPS.2017.115>
 - [27] MVAPICH TEAM. 2020. MVAPICH2-X 2.3 User Guide. <https://mvapich.cse.ohio-state.edu/static/media/mvapich/mvapich2-x-userguide.pdf>
 - [28] Rajeev Thakur, Rolf Rabenseifner, and William Gropp. 2005. Optimization of collective communication operations in MPICH. *The International Journal of High Performance Computing Applications* 19, 1 (2005), 49–66.
 - [29] R. Underwood, S. Di, J. C. Calhoun, and F. Cappello. 2020. FRaZ: A Generic High-Fidelity Fixed-Ratio Lossy Compression Framework for Scientific Floating-point Data. In *2020 IEEE International Parallel and Distributed Processing Symposium (IPDPS)*. IEEE Computer Society, Los Alamitos, CA, USA, 567–577. <https://doi.org/10.1109/IPDPS47924.2020.00065>
 - [30] Yusong Wang and Michael Borland. 2006. Pelegant: A parallel accelerator simulation code for electron generation and tracking. In *AIP Conference Proceedings*, Vol. 877. American Institute of Physics, 241–247.
 - [31] Xin-Chuan Wu, Sheng Di, Emma Maitreyee Dasgupta, Franck Cappello, Hal Finkel, Yuri Alexeev, and Frederic T. Chong. 2019. Full-State Quantum Circuit Simulation by Using Data Compression. In *Proceedings of the International Conference for High Performance Computing, Networking, Storage and Analysis (Denver, Colorado) (SC '19)*. Association for Computing Machinery, New York, NY, USA, Article 80, 24 pages. <https://doi.org/10.1145/3295500.3356155>
 - [32] Annie Yang, Hari Mukka, Farbod Hesaaraki, and Martin Burtcher. 2015. MPC: A Massively Parallel Compression Algorithm for Scientific Data. (2015).
 - [33] Xiaodong Yu, Sheng Di, Kai Zhao, Jiannan Tian, Dingwen Tao, Xin Liang, and Franck Cappello. 2022. Ultrafast Error-Bounded Lossy Compression for Scientific Datasets. In *Proceedings of the 31st International Symposium on High-Performance Parallel and Distributed Computing (Minneapolis, MN, USA) (HPDC '22)*. Association for Computing Machinery, New York, NY, USA, 159–171. <https://doi.org/10.1145/3502181.3531473>
 - [34] Kai Zhao, Sheng Di, Maxim Dmitriev, Thierry-Laurent D. Tonellot, Zizhong Chen, and Franck Cappello. 2021. Optimizing Error-Bounded Lossy Compression for Scientific Data by Dynamic Spline Interpolation. In *2021 IEEE 37th International Conference on Data Engineering (ICDE)*. 1643–1654. <https://doi.org/10.1109/ICDE51399.2021.00145>
 - [35] Kai Zhao, Sheng Di, Xin Lian, Sihuan Li, Dingwen Tao, Julie Bessac, Zizhong Chen, and Franck Cappello. 2020. SDRBench: Scientific Data Reduction Benchmark for Lossy Compressors. In *2020 IEEE International Conference on Big Data (Big Data)*. 2716–2724.
 - [36] Kai Zhao, Sheng Di, Xin Liang, Sihuan Li, Dingwen Tao, Zizhong Chen, and Franck Cappello. 2020. Significantly improving lossy compression for HPC datasets with second-order prediction and parameter optimization. In *Proceedings of the 29th International Symposium on High-Performance Parallel and Distributed Computing*. 89–100.
 - [37] Kai Zhao, Sheng Di, Danny Perez, Xin Liang, Zizhong Chen, and Franck Cappello. 2022. MDZ: An Efficient Error-bounded Lossy Compressor for Molecular Dynamics. In *2022 IEEE 38th International Conference on Data Engineering (ICDE)*. 27–40. <https://doi.org/10.1109/ICDE53745.2022.00007>
 - [38] Q. Zhou, C. Chu, N. S. Kumar, P. Kousha, S. M. Ghazimirsaeed, H. Subramoni, and D. K. Panda. 2021. Designing High-Performance MPI Libraries with On-the-fly Compression for Modern GPU Clusters. In *2021 IEEE International Parallel and Distributed Processing Symposium (IPDPS)*. 444–453. <https://doi.org/10.1109/IPDPS49936.2021.00053>
 - [39] Qinghua Zhou, Pouya Kousha, Quentin Anthony, Kawthar Shafie Khorassani, Amir Shafi, Hari Subramoni, and Dhabaleswar K. Panda. 2022. Accelerating MPI All-to-All Communication With Online Compression On Modern GPU Clusters. In *High Performance Computing: 37th International Conference, ISC High Performance 2022, Hamburg, Germany, May 29 – June 2, 2022, Proceedings* (Hamburg, Germany). Springer-Verlag, Berlin, Heidelberg, 3–25. https://doi.org/10.1007/978-3-031-07312-0_1